JOURNAL OF VIROLOGY, Nov. 2000, p. 10430–10437 Vol. 74, No. 22
0022-538X/00/$04.00+0

Hepatitis C Virus Internal Ribosome Entry Site (IRES) Stem Loop IIId Contains a Phylogenetically Conserved GGG Triplet Essential for Translation and IRES Folding

RONALD JUBIN,[1] NICOLE E. VANTUNO,[1] JEFFREY S. KIEFT,[2] MICHAEL G. MURRAY,[1] JENNIFER A. DOUDNA,[2,3] JOHNSON Y. N. LAU,[1] AND BAHIGE M. BAROUDY[1]*

Department of Antiviral Therapy, Schering-Plough Research Institute, Kenilworth, New Jersey 07033,[1] and Department of Molecular Biophysics and Biochemistry[3] and Howard Hughes Medical Institute,[2] Yale University, New Haven, Connecticut 06520

Received 27 March 2000/Accepted 18 August 2000

The hepatitis C virus (HCV) internal ribosome entry site (IRES) is a highly structured RNA element that directs cap-independent translation of the viral polyprotein. Morpholino antisense oligonucleotides directed towards stem loop IIId drastically reduced HCV IRES activity. Mutagenesis studies of this region showed that the GGG triplet (nucleotides 266 through 268) of the hexanucleotide apical loop of stem loop IIId is essential for IRES activity both in vitro and in vivo. Sequence comparison showed that apical loop nucleotides (UUGGGU) were absolutely conserved across HCV genotypes and the GGG triplet was strongly conserved among related *Flavivirus* and *Pestivirus* nontranslated regions. Chimeric IRES elements with IIId derived from GB virus B (GBV-B) in the context of the HCV IRES possess translational activity. Mutations within the IIId stem loop that abolish IRES activity also affect the RNA structure in RNase T_1-probing studies, demonstrating the importance of correct RNA folding to IRES function.

Hepatitis C virus (HCV) is a member of the genus *Hepacivirus* in the *Flaviviridae* family (8). HCV infection is a global health problem, with chronically infected patients exhibiting an increased risk for the development of cirrhosis and hepatocellular carcinoma (19). HCV has a single-strand, positive-sense RNA genome known for its genetic heterogeneity, and HCV has been classified into six major genotypes and a series of subtypes (30, 31). However, the 5′ nontranslated region (5′NTR) of the virus is relatively well conserved among all genotypes (5, 9).

Located within the 5′NTR is the internal ribosome entry site (IRES) previously shown to contain sequence and structural elements responsible for directing cap-independent translation of the viral polyprotein (36, 38). Stem-loop I had been previously shown not to be essential for IRES activity (17, 27, 28). Based on a number of published reports, the minimal sequence required for IRES activity is believed to include nucleotide sequences spanning nucleotides (nt) 42 through 356 (12–14, 26–28). Within the minimal IRES sequence, three primary structured domains, known as stem-loops II, III, and IV, have been identified based on chemical and enzymatic probing as well as phylogenetic comparisons (4, 13, 14, 20, 40). Each primary domain of the IRES is further defined based on a combination of double-stranded (ds) helices and single-strand bulges or loops. A number of studies have been conducted to determine the importance of some of these structured elements in viral translation, including the pseudoknot and stem-loops II, IIIb, IIIc, IIIe, and IV (12–14, 17, 25, 27–29, 35, 39, 40). In general, mutations altering double-stranded helical regions can have deleterious effects on translation. However, when compensatory mutations are made to restore Watson-Crick base pairing, the translation efficiency can often be restored. In contrast, mutational changes in loop regions appear to be more amenable and may retain IRES activity (39). Recently, it has also been demonstrated that domains IIIb to IIIc are involved in the binding to eukaryotic initiation factor 3a and the 40S ribosomal subunit (6, 23, 32). These studies suggested that the HCV IRES contains sequence- and structure-specific elements that are essential for IRES activity.

Domain III of the HCV IRES has six distinct regions containing stem-loop structures (a through f) according to previously proposed secondary-structure models (4, 13). Stem-loop IIId is a highly conserved region of domain III spanning nucleotides 253 through 279. It is composed of two double-stranded helical (1 and 2) elements separated by a 3-nucleotide internal asymmetric loop with a 6-nucleotide hairpin loop at the distal end of double-stranded helix 2 (Fig. 1C). Large deletions of HCV IRES sequences including stem-loop IIId have been previously shown to be detrimental to IRES function (12, 28).

The aim of the present study was to examine the specific role of stem-loop IIId in HCV IRES translation by a combination of techniques including antisense studies, mutagenesis, and the assembly of chimeric IRESs. RNase T_1 protection assays were subsequently conducted to probe the structural changes induced by point mutations and chimeric IRES elements.

MATERIALS AND METHODS

Plasmids. The HCV IRES element derived from genotype 1b was obtained from plasmid pK1b (kindly provided by A. Nomoto). To facilitate cloning, plasmid pK1bE was constructed by modifying the sequences preceding the IRES element through the annealing of two partially complementary synthetic oligonucleotides (S-ONs) (Life Technologies, Gaithersburg, Md.) (5′-GCGCCAGC CCC-3′ and 5′-GGGCTGGCGC-3′) introduced into the *Xba*I-Klenow and *Xcm*I restriction sites. This allowed for the introduction of an *Ehe*I restriction site at nucleotide 1 of the HCV IRES. A similar approach was adopted for the modification of the core sequences using two partially complementary oligonucleotides (5′-CGGCGCCACGT-3′ and 5′-GGCGCCGACGT-3′) into the *Aat*II restriction site. Again this created an *Ehe*I restriction site. Hence, an *Ehe*I cassette plasmid (pK1BE/E) containing HCV nucleotides 1 through 408 with three additional nucleotides at the 3′ end (GGC) was established.

Stem loop IIId mutants were constructed by insertion of annealed S-ONs

* Corresponding author. Mailing address: Antiviral Therapy K-15-4945, Schering-Plough Research Institute, 2015 Galloping Hill Rd., Kenilworth, NJ 07033. Phone: (908) 740-3046. Fax: (908) 740-3918. E-mail: bahige.baroudy@spcorp.com.

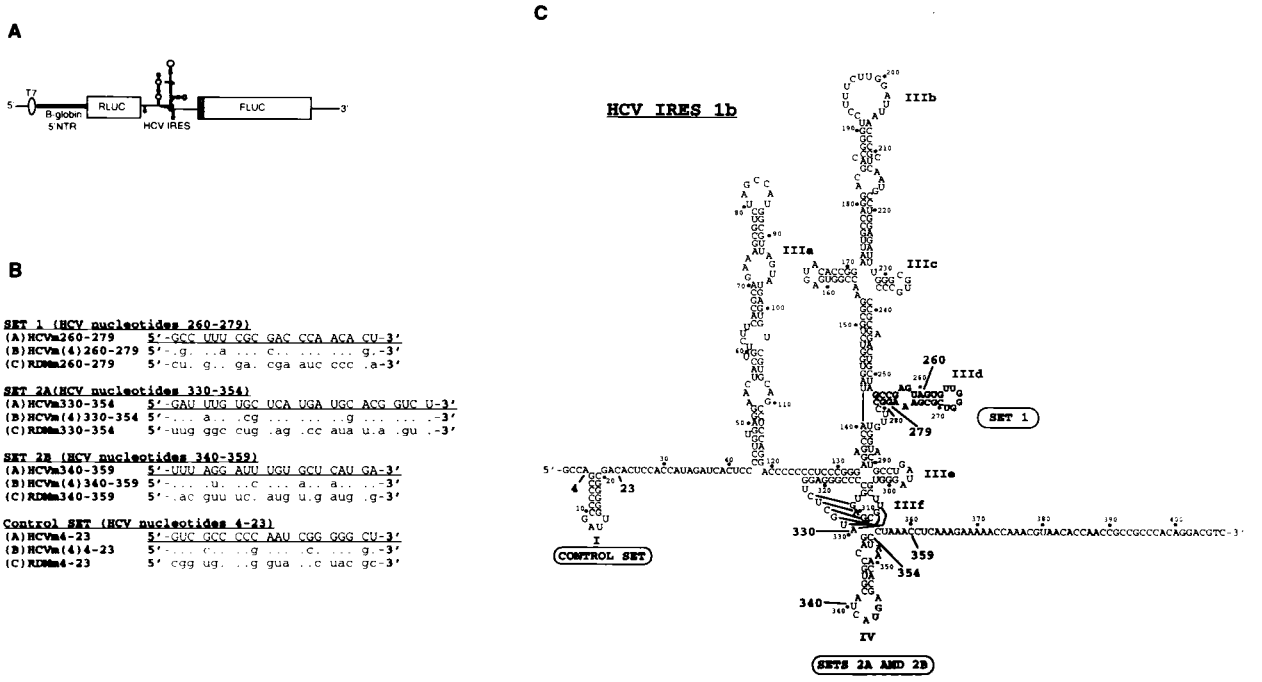

FIG. 1. (A) Schematic representation of plasmid used for analysis containing the HCV IRES. T7 is the location of the T7 RNA polymerase promoter sequences for transcription of bicistronic RNA. Reporter RLUC is under translational control of the *Xenopus* β-globin 5′NTR while ΔCore (hashed box)/FLUC is under translational control of the HCV IRES as described in Materials and Methods. (B) Morpholino antisense oligonucleotides used for antisense inhibition studies. Antisense nucleotide sequences are listed in underlined text within each set, while mismatch controls are listed below. Dots represent identical sequences, while lowercase letters denote base pair substitutions. m(4) denotes a 4-bp mismatch, and RDM indicates random sequences. (C) Secondary model of the HCV IRES (15), including all sequences (nucleotides 1 through 408) used to construct the assay plasmid shown in panel A. Locations of the antisense targets are shown with oval boxes. IIId loop nucleotides 253 through 279 and numbers corresponding to antisense target sequences are shown in bold type.

containing mutations into the *Nhe*I and *Stu*I restriction sites that span the stem loop. Plasmid DNA was purified using Maxiprep kits (Qiagen, Valencia, Calif.), and all sequences were confirmed by restriction analysis and primer extension automated DNA sequencing (ABI PRISM 377 DNA sequencer; Perkin-Elmer, Norwalk, Conn.).

Bicistronic plasmids were constructed to determine HCV IRES activity in relation to cap-dependent translation. Bicistronic constructs were generated by first assembling a cassette vector containing the *Renilla* (*RLUC*) and firefly (*FLUC*) luciferase genes as cistrons 1 and 2, respectively. Plasmid pGL3-control (Promega, Madison, Wis.) containing *FLUC* was modified to remove the initiator codon AUG and introduce an *Sna*BI restriction site at its 5′ terminus. Two S-ONs, 5′-AGCTTACGTAGAAGACGCCAAAAACATAAAGAAAGGCCC GGC-3′ and 5′-GCCGGGCCTTTCTTTATGTTTTTGGCGTCTTCTACGTA-3′, were annealed and introduced into *Hin*dIII and *Ehe*I restriction sites. This insertion replaces the initiator methionine codon with a valine codon (pGL3CHV). The *Xba*I restriction site in the vector sequence was eliminated to simplify additional cloning steps by restricting pGL3CHV with *Xba*I-Klenow and religating [pGL3CHV(-X)]. Plasmid pT7βRL containing the T7 promoter, *Xenopus* β-globin 5′NTR, and the *RLUC* gene was restricted with *Sma*I-*Sna*BI and religated to delete the *Sna*BI restriction site [pT7βRL(-s/s)] (16). The bicistronic cassette vector containing the *RLUC* gene 5′ of the *FLUC* gene was constructed by cloning the *Hin*dIII/*Bam*HI-Klenow-treated fragment of pGL3CHV(-X), which contains the *FLUC* gene, simian virus 40 poly(A) signal, and enhancer sequences, into pT7βRL(-s/s) restricted with *Xba*I-Klenow resulting in pT7βR-P(a). HCV IRES sequences were isolated from pK1BE/E by restriction digestion with *Ehe*I and annealed in frame with the *FLUC* gene of pT7βR-P(a) restricted with *Xba*I-Klenow and *Sna*BI, creating pT7βR(1b/408)P. This plasmid was used for simultaneous monitoring of cap-dependent and IRES-mediated translation (Figure 1A). Stem-loop IIId mutations were transferred into the bicistronic plasmid by swapping the *Nco*I-*Acc*I fragments from the monocistronic plasmids into the same restriction sites in pT7βR(1b/408)P.

An encephalomyocarditis viral (EMCV) bicistronic plasmid was prepared to serve as an HCV IRES specificity control in antisense studies. pCITE-4a (Novagen, Milwaukee, Wis.), a vector containing an EMCV IRES, was modified by inserting two annealed S-ONs, 5′-TAGAAGACGCCAAAAACATAAAGAAA GGCCCGGCGCC-3′ and 5′-GGCGCCGGGCCTTTCTTTATGTTTTTGGC GTCTTCTA-3′, into the *Msc*I restriction site, which contained sequences that overlapped the 3′ portion of the EMCV IRES and the 5′ end of the *FLUC* gene. The resulting plasmid pCITE-4aΔLUC(E) facilitated cloning the EMCV IRES in frame with the *FLUC* gene. pT7BR(EMCV)P was created by cloning the 543-bp *Bsa*WI-*Ehe*I fragment containing the EMCV IRES into pT7BR-P(a) restricted with *Xba*I-Klenow and *Ehe*I.

In vitro transcription and translation. In vitro transcription and translation reactions were carried out using the TNT coupled transcription-translation system (Promega, Madison, Wis.). Duplicate reaction mixtures (25 μl) were assembled containing 19.5 μl of rabbit reticulocyte lysate (RRL) master mixture and 0.5 μl of methionine (1 mM) and were programmed with 5.0 μl of purified plasmid DNA (0.1 μg/μl) in Microlite 2 microtiter plates (Dynex, Chantilly, Va.). Following the combination of reaction mixture components, samples were incubated at 30°C for 90 min. Postincubation, RRL reactions were analyzed for both RLUC and FLUC reporter activities using the Dual-Luciferase reporter assay system (Promega) according to the manufacturer's instructions and quantitated with a luminometer (model MLX; Dynex). The relative translational efficiency in mutational-analysis experiments was determined by comparing FLUC/RLUC ratios of mutation samples to native IRES reactions.

Antisense studies. Translation reactions were carried out as described above except that morpholino antisense oligonucleotides or mismatch controls (Anti-Virals, Corvallis, Oreg.) were added to a 50-μl reaction mixture (39 μl of RRL master mixture, 1.0 μl of methionine, 5.0 μl of DNA, and 5.0 μl of 10× morpholino oligonucleotide). Relative levels of IRES translational inhibition in antisense studies were determined for each reporter independently, and percent inhibition was determined by comparison of samples with morpholino antisense oligonucleotides to control samples.

In vivo cell culture studies. BT7-H cells that constitutively express T7 polymerase were maintained in Dulbecco's modified eagle medium (DMEM) containing 10% fetal calf serum, 100 U of penicillin and streptomycin per ml, 5 ml of nonessential amino acids, and 500 μg of G418 sulfate per ml (14). Cells were seeded into 96-well tissue culture dishes at a density of 1.2×10^4 cells/well and incubated overnight at 37°C in 5% CO_2. DNA transfections were carried out in duplicate using 1.0 μl of plasmid DNA (0.1 μg) and Lipofectamine Plus transfection reagents (Life Technologies) according to the manufacturer's protocol. Cells were washed, and medium was replaced with a 60-μl mixture containing 1.0 μl of DNA, 1.0 μl of Plus reagent, and 0.5 μl of Lipofectamine in DMEM without supplements and incubated for 3 h at 37°C and 5% CO_2. Following incubation, the medium was removed by aspiration and replaced with complete medium and returned to the incubator for an additional 18 h. Subsequently, the cells were lysed in 25 μl of 1× passive lysis buffer and assayed using the Dual-Luciferase assay system (Promega). Cell lysate (20 μl) was transferred to Microlite 2 96-well plates and placed into the luminometer. Luciferase activities were analyzed in a fashion identical to that for in vitro samples except that

luciferase substrate mixtures were added by microinjection followed by reporter activity quantitation as described above.

RNase T_1 probing. HCV IRES RNAs including nucleotides 40 through 372 were transcribed from linearized plasmid DNA, purified, and subjected to RNase T_1 enzyme as previously described (18). Briefly, 5′-end-labeled RNA was heated to 65°C for 1 min and then cooled to room temperature. This annealed RNA was added to a tube containing buffer (final concentration, 30 mM *N*-2-hydroxyethyl piperazine-*N*′-2-ethanesulfonic acid [HEPES; pH 7.5]), 1.0 μg of tRNA, and the desired divalent ion to a final volume of 9.0 μl. RNA was incubated at 37°C for 5 min to achieve folding equilibrium. Cleavage was initiated by addition of 1.0 μl of RNase T_1 (0.1 U/μl; Boehringer Mannheim), incubated at 37°C for 7 min, then quenched with the addition of 10.0 μl of 9 M urea–1 mM EDTA, and placed on ice. Reaction mixtures were resolved on 10% polyacrylamide gels that were dried and visualized on a PhosphorImager.

RESULTS

RNase H-independent antisense oligonucleotides directed to stem-loop IIId drastically reduce IRES activity. Inhibition studies of the HCV IRES IIId region were carried out using morpholino antisense oligonucleotides which have been previously shown to work in an RNase H-independent fashion (33, 34). Loss of translation efficiency by hybridization arrest might indicate whether loop IIId interactions are important for IRES function. As shown in Fig. 1B and C, four separate sets of morpholino antisense oligonucleotides spanning HCV nucleotides 260 through 279 (set 1), 330 through 354 (set 2A), 340 through 359 (set 2B), and 4 through 23 (control set) were synthesized. For each region targeted, two additional control oligonucleotides were also synthesized that contained either 4-bp mismatches or random rearrangement of the target nucleotide sequences. Morpholino antisense oligonucleotides directed to the region spanning the initiator AUG (sets 2A and 2B) showed dramatic reduction of FLUC (IRES-mediated) activities (>80%) with low (<22%) inhibition of the upstream RLUC (cap control) activities (Fig. 2A). Set1A, which spans stem loop IIId, exhibited inhibitory values comparable to sets 2A and 2B. Control set oligonucleotides directed to sequences situated 5′ of the minimal IRES (nt 43 through 356) exhibited no inhibition of IRES activity. Furthermore, the control morpholino antisense oligonucleotides for each individual set (4-bp mismatch and random) showed no specific inhibition of the HCV IRES. In addition, set 1 exhibited a dose-dependent inhibition of the HCV IRES-mediated translation and exerted no inhibitory effects on the translational efficiency of the EMCV IRES (Fig. 2B), demonstrating that inhibition was HCV IRES specific and did not affect reporter activities. Based on the specific inhibition of IRES activity exhibited by set 1 and the absolute sequence conservation of HCV nucleotides spanning 264 through 269, we proceeded to carry out mutational analysis of this apical loop to determine which nucleotides are essential for IRES activity.

Dramatic changes in the apical loop of IIId severely reduce IRES activity. Mutational in vitro studies of the apical loop of IIId were conducted, including sequence deletions, complements, and inversions, to assess the requirements of this region for IRES translational activities. As shown in Fig. 3, a mutation containing complete deletion of nucleotides spanning the apical loop (LD-SD) totally abolished IRES activity that demonstrated the importance of this loop structure for translational activity. Two additional mutations that maintained the loop structure, but created partial (LD-SM) or total sequence complement (LC-SC) mutations produced similar results, which suggested that primary sequence requirements were also important for IRES function. Finally, a mutation containing the loop sequence in 3′ to 5′ orientation (LC-SV) was analyzed, which produced moderate activity (37%) of the IRES. Correspondingly, the activities of all mutations were similar to the in vivo cell-based study results. Therefore, in an effort to map

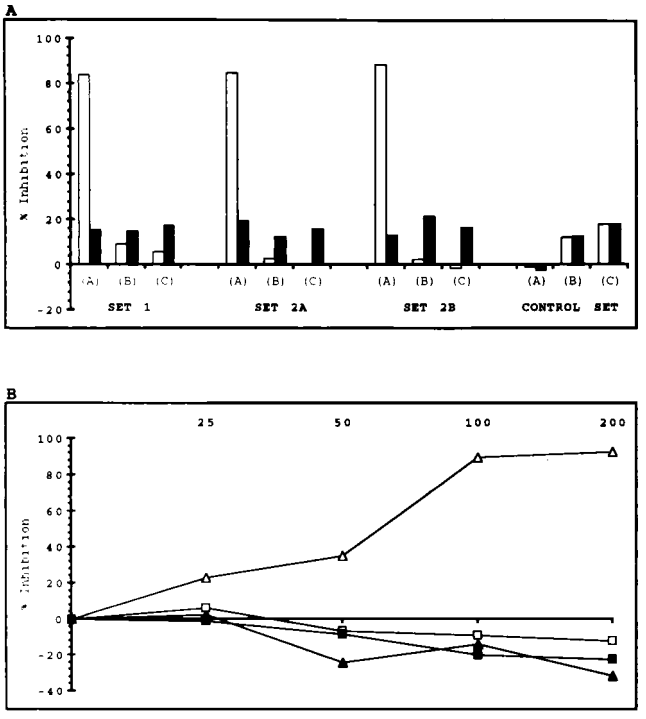

FIG. 2. Morpholino antisense inhibition of the HCV IRES. (A) Equal concentrations (200 nM) of various antisense oligonucleotides (see Fig. 1B) were included in coupled TNT transcription/translation reactions programmed with pT7βR(1b/408)P. Percents inhibition were determined by direct comparison of antisense oligonucleotide-containing samples to control reaction samples without antisense addition. Open bars represent FLUC (IRES) inhibition; shaded bars represent RLUC inhibition. (B) HCVm260-279 antisense oligonucleotides were added to TNT transcription-translation reactions at assay concentrations ranging from 25 to 200 nM. Triangles represent pT7βR(1b/408)P; squares represent pT7βR(EMCV)P. Open figures illustrate FLUC (IRES) inhibition patterns; shaded figures represent RLUC inhibition of each respective assay plasmid.

IRES efficiency at the individual-nucleotide level, a series of systematic point mutations were assembled for analysis in the bicistronic system.

Point mutations of the apical loop produce various levels of inhibition of HCV IRES. Single-nucleotide mutations with complementary-nucleotide substitutions were systematically introduced into the IIId apical loop nucleotides (spanning nucleotides 264 through 269 [Fig. 4A]) and analyzed in the bicistronic system. Translational activities of point mutations exhibited varied levels of IRES translational efficiency. The U-A complementary mutations (U264A, U265A, and U269A) exhibited strong translational activities in RRL assays (75, 58, and 85%, respectively) and, in the cell-based studies, they all showed similar translational activities of ~43%, suggesting the necessity of these nucleotides in the more stringent cell-based system. In contrast, all G-C complementary mutations (G266C, G267C, and G268C) showed >95% reduction in both RRL and in vivo cell-based assays (Fig. 4B). Concurrently, a set of G-C mutations containing multiple substitutions was also analyzed, which displayed results similar to those with single substitutions (Fig. 4C and D). Similar results were confirmed in monocistronic assays comparing HCV core expression and also in RNA bicistronic translation assays (reference 18 and data not shown). These data indicated that U nucleotides in the IIId apical loop are important for optimal IRES function and that each G nucleotide was absolutely essential for IRES translation.

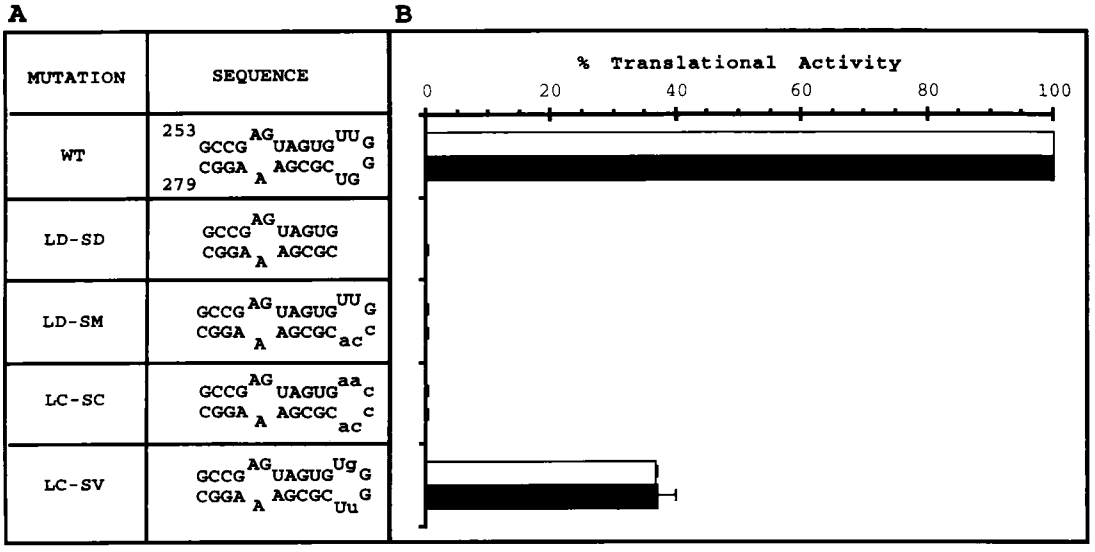

FIG. 3. Mutational analysis of the HCV IRES IIId apical loop. (A) Specific IIId apical loop mutations and secondary structures. Nucleotide substitutions are denoted by lowercase letters, with wild-type (WT) IIId sequences and structures listed at the top for comparison. Abbreviations: LD, loop deleted; LC, loop conserved; SD, sequence deleted; SM, semimaintained; SC, sequence complementary; SV, sequence varied 3′ to 5′. (B) Wild-type bicistronic plasmid DNA or plasmid DNA samples containing mutations were used to program in vitro-coupled transcription-translation RRL reactions or were transfected into BT7-H cells. Relative IRES efficiencies were determined for each mutation by direct comparison of FLUC/RLUC ratios to wild-type values (arbitrarily 100%). Open bars represent in vitro RRL mean IRES efficiencies; shaded bars represent the same from BT7-H cell-based transfections. Duplicate samples were analyzed in three separate experiments; error bars represent standard errors of the mean.

Sequence alignment of stem-loop IIId shows that the GGG triplet is conserved among HCV genotypes and related viruses. Secondary-structure predictions of *Flavivirus* and *Pestivirus* have previously shown that the IIId stem-loop is present in several related viral IRES elements (20). To determine whether these IIId loops also contained conserved sequences similar to those of HCV, an alignment analysis was conducted with several related viruses. First, several HCV isolates, one from each of the six genotypes of HCV, were aligned to the HCV 1b IIId sequences used in this present study (Fig. 5). The UUGGGU sequences comprising the entire apical loop are absolutely conserved among all genotypes listed, and the majority of the double-stranded helix and internal asymmetric loop sequences are also highly conserved except for a double covariant substitution, U262C and C270U. Further alignments pairing the GGG triplet of the IIId region with the related GB virus B (GBV-B) *Flavivirus* shows the UUGGG sequences are conserved, however secondary structure models predict that the UU pair is absent from the apical loop (14). The pestiviruses, bovine viral diarrhea virus (BVDV) and classical swine fever virus (CSFV) were also aligned and showed conservation of the GGG triplet and GGGU sequences, respectively. Based on these alignment profiles and previously predicted secondary structures, it is apparent that apical loop IIId is conserved among related viruses with the GGG triplet being absolutely conserved.

These sequence and mutational data strongly support the critical requirements of nucleotides G266, G267, and G268 for HCV IRES activity, thus suggesting the possibility of a similar importance in related viruses. To test this hypothesis, chimeric IRES elements were assembled containing substitution of the HCV IIId region with those of GBV-B, a related virus, and the HIV-1 Tar element, an unrelated viral NTR region containing a GGG triplet in an apical loop (15).

Chimeric HCV IRESs containing a GBV-B IIId can support IRES activity. A chimeric IRES that contained a major portion of the GBV-B stem-loop IIId was introduced into the *Nhe*I and *Stu*I sites of the HCV IRES (Fig. 6A). Comparison of the chimeric HCV/IIId-GBV-B (GBV-B1) chimera with the native bicistronic construct exhibited an in vitro activity of 32% (Fig. 6B). Two additional mutations were subsequently constructed that incorporated structural features unique to the HCV IRES into the GBV-B stem-loop in attempts to improve translation. First, the internal asymmetric loop of HCV IIId was introduced into the GBV-B sequence (GBV-B2). Second, the UU pair (HCV nt 264 through 265) was added preceding the GGG triplet, thus creating an identical HCV apical loop with a GBV-B ds helix (GBV-B3) (Fig. 6A). Unexpectedly, introduction of the internal asymmetric loop completely abolished IRES activity. In contrast, removal of the internal asymmetric loop from wild-type HCV IIId resulted in a dramatic loss of IRES activity (data not shown). The addition of the UU moderately enhanced activity (32 to 43%) in the in vitro studies (Fig. 6B). Levels of the two active GBV-B chimeras (B1 and B3) showed similar in vivo results (~18%). We also constructed and analyzed in parallel a human immunodeficiency virus type 1 (HIV-1) Tar loop chimera that possesses a secondary structure similar to HCV IIId and also contains a GGG in its apical loop (Fig. 6A). IRES activity was severely limited (<10%) in either the in vitro or in vivo cell-based assays with the HCV/Tar-HIV-1 chimera (Fig. 6B).

Structural analysis of chimeric mutants. Enzymatic probing with RNase T_1 has been previously employed to monitor the ion-dependent folding of the HCV IRES (18). We used this technique to determine the changes in RNA structure that accompany the introduction of chimeric sequences into the HCV IRES. Figure 7 shows the cleavage patterns of wild-type HCV IRES RNA and the three GBV-B chimeras, in the absence and presence of 2.5 mM magnesium. Both GBV-B1 and GBV-B3 have protection patterns similar to that of the wild type in both the absence and presence of the divalent ion (lanes 4, 5, 8, 9, 16, 17). The chimeras differ only slightly from the wild type in that the apical loop GGG sequence is cut somewhat more strongly in the absence of magnesium ion. In

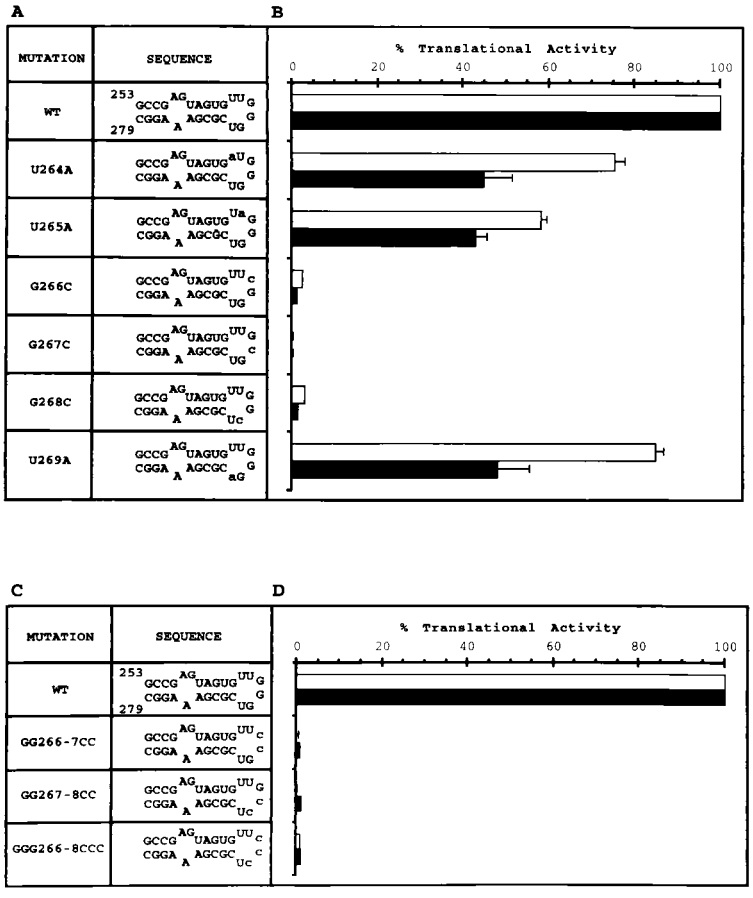

FIG. 4. Mapping of IIId nucleotides essential for IRES translation. (A and C) Specific IIId apical loop mutations and secondary structures. Nucleotide substitutions are denoted by lowercase letters, with wild-type (WT) IIId sequences and structures listed at the top for comparison. (B and D) Relative IRES translational efficiencies of point or multiple G mutations, respectively, were determined as described in the legend to Fig. 3. Open bars, in vitro RRL mean IRES efficiencies; shaded bars, the same from BT7-H cell-based transfections.

contrast, the translationally inactive GBV-B2 chimera has an RNase T_1 protection pattern that clearly differs from the wild type irrespective of ionic conditions (lanes 12 and 13). Specifically, positions G253 and G255 are cleaved strongly in the absence of magnesium, while G nucleotides both up- and downstream that are cut in the wild-type sequence are protected in GBV-B2 (G258 through 267 and G243 through 249). In the presence of magnesium, this pattern changes dramatically. The G nucleotides in the apical loop are strongly cut, but the G nucleotides upstream of this loop (G245 through G255) are now susceptible to cleavage.

Probing of mutants U264A, U265A, and U269A by RNase T_1 did not reveal any changes in the cleavage patterns of these sequences, relative to wild-type IRES (data not shown). This indicated that these mutations did not induce a detectable change in the RNA structure. The effects of G-C mutations of apical loop nucleotides 266 through 268 on the RNase T_1 protection pattern have been reported elsewhere (18).

DISCUSSION

Antisense oligonucleotides directed to the HCV IRES have been previously employed to inhibit IRES activity (1, 7, 11, 21, 37). Most antisense approaches such as phosphorothioate chemistry elicit the cellular enzyme RNase H to the double-stranded target region and invoke enzymatic cleavage of the RNA substrate. Morpholino oligonucleotides contain a six-member morpholino backbone in place of the natural riboside moiety which is not recognized by RNase H (2, 34). The present study demonstrated that hybridization arrest of translation with morpholino antisense oligonucleotides in an RRL in vitro assay can be useful in identifying potentially important regions of an IRES element located at a distance from the translational start site. Specifically, these data showed that translational inhibition as a result of blocking IIId was possibly

253	GCCGAGUAGUGUUGGGUCGCGAAAGGC	279	1b	accession #
	***			
253	.....	279	1a	AF009606
253	.....c.....u.....	279	2a	D31605
253	.....	279	3a	AF046866
253	.....	279	4a	Y11604
253	.....	279	5a	Y13184
253	.....c.....u.....	279	6a	Y12083
363	----g.au.gu.g....uagcc.ucc-	384	GBV-B	U22304
268	----.ccu.a.cg...gucgcccaggu	290	BVDV	M31182
257	-uuacccu.gcgg.....u.gg.ug	283	CSFV	AF091507

FIG. 5. IIId stem-loop sequence alignment of HCV genotypes 1 through 6, related *Flavivirus* GBV-B, and pestiviruses BVDV and CSFV. Nucleotide numbers in viral genomes are listed along with genotype and accession number (GenBank). HCV IRES genotype 1b used in this study is underlined at the top, with the conserved GGG triplet identified by asterisks. Listed below genotype 1b are the sequence alignments. Identical sequences are represented by dots, and nucleotide variations are indicated by lowercase letters, while dashes denote gaps in alignments.

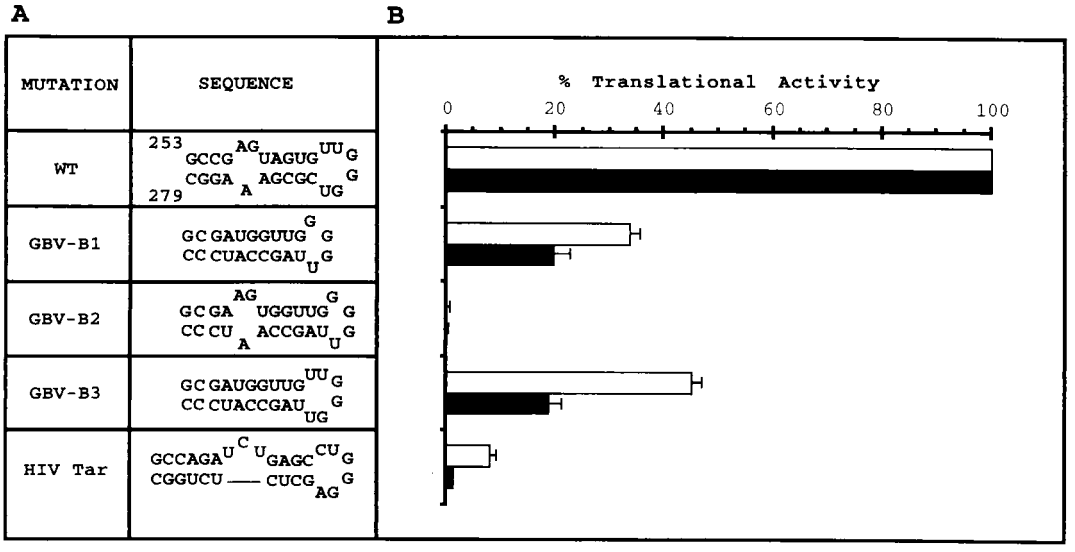

FIG. 6. Chimeric substitutions and effects on relative IRES translation. (A) Specific IIId apical loop mutations and secondary structures. Nucleotide substitutions are denoted by lowercase letters, with wild-type (WT) IIId sequences and structures listed at the top for comparison. (B) Relative IRES translational efficiencies of chimeric IRESs were determined as described in the legend to Fig. 3. Open bars represent in vitro RRL mean IRES efficiencies; shaded bars represent the same from BT7-H cell-based transfections.

a result of IRES destabilization or that it prevented essential RNA-protein and/or RNA-RNA interactions.

Mutational analysis was subsequently used to determine whether specific IIId nucleotide sequences were important for maintaining translational efficiency of the HCV IRES. Overall, these results implied that both the loop nucleotide sequence and local structure were important aspects for maintaining IRES activity. Further definition of critical nucleotides in the

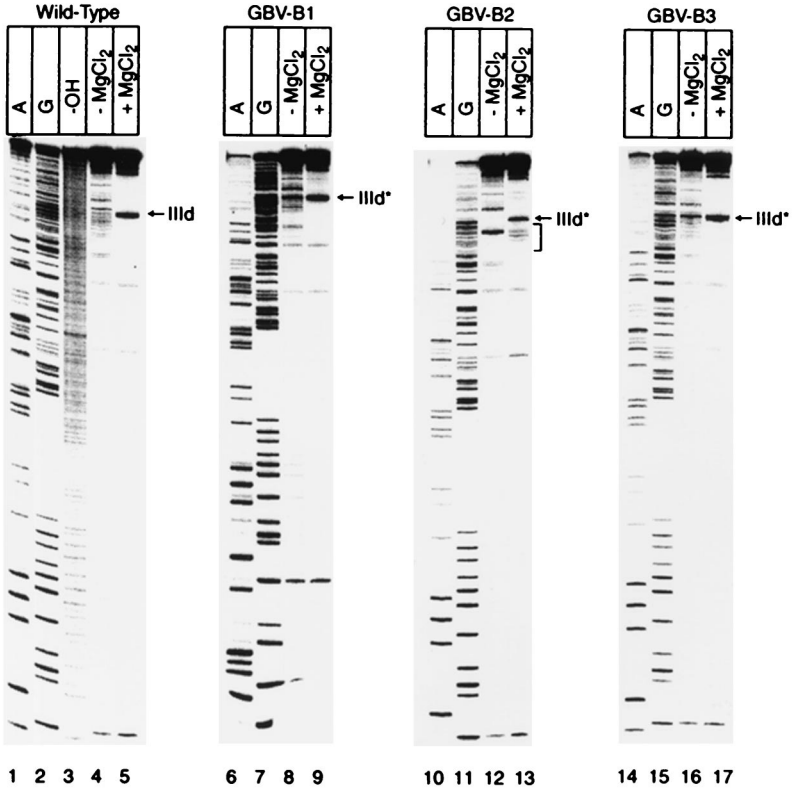

FIG. 7. RNase T_1 probing of wild-type HCV IRES and GBV-B/HCV chimeric RNA in the absence (−) and presence (+) of 2.5 mM $MgCl_2$. Addition of $MgCl_2$ resulted in cleavage patterns similar to wild-type HCV for GBV-B1 and GBV-B3 (lanes 5, 9, and 17) but different for GBV-B2 (lane 13). The location of the IIId apical loop is indicated by an arrow, and the asterisks indicate chimeric loops. A bracket indicates the region of GBV-B2 that was most different from others. This region corresponded to loop IIId and upstream regions extending to G243. Lanes 1, 2, and 3 contain an RNase U_2 sequencing ladder (denaturing conditions), an RNase T_1 sequencing ladder (denaturing conditions), and a hydrolysis ladder, respectively. These samples were not all run on the same gel; therefore, the run times differ slightly.

IIId apical loop was accomplished by complementary single-nucleotide substitutions that showed an essential requirement for each G nucleotide (266 through 268) (Fig. 4). Parallel studies with multiple G substitutions produced similar results, suggesting that G-C mutation inhibition profiles are not additive but instead that there is a critical requirement of each individual G nucleotide for IRES activity. In contrast, the U-A (nucleotides 264, 265, and 269) mutations did not drastically impair IRES function.

Sequence profiles aligning the IIId loops of different HCV genotypes and related GBV-B, BVDV, and CSFV showed that apical loop GGG trinucleotide sequences are conserved among these different viral IRESs. Recently it has been shown that loop sequences in domain II of GBV-B and HCV are highly conserved (14). To ascertain whether conservation of apical loop sequences from these related viruses was attributable to comparable roles in translation, chimeric IRESs were assembled containing GBV-B IIId sequences (Fig. 6A). Although GBV-B IIId sequences can support HCV IRES translation in vitro, both GBV-B1 and GBV-B3 translational activities were reduced by approximately 50% in cell-based assays (Fig. 6B). These apparent differences between in vitro and in vivo results were also observed in U-A mutations described earlier and may indicate different stringencies for each assay system or strict intracellular requirements for translation that are absent in the RRL system.

Lack of total recovery of IRES activity in GBV-B chimeras could be due to inherent differences, unique to each IRES, that developed during viral evolution. For example, examination of IIId stem loop sequences of HCV compared to those of GBV-B and related pestiviruses shows distinct differences (Fig. 5; 20, 24, 32). GBV-B lacks the internal asymmetric loop whereas BVDV and CSFV actually contain two IIId loops (IIId and IIId′) with IIId containing a symmetric bulge between helical regions. Even the apical loops of each IRES IIId stem-loop contain a unique arrangement as indicated by secondary-structure predictions. However, similar functions of BVDV and CSFV IRESs are supported by recent reports that have shown comparable requirements for translation initiation factors compared to the HCV IRES (24, 32). Moreover, it also has been recently shown that an HCV/BVDV chimeric virus that contains the HCV IRES is capable of viral translation and replication (10). Thus, nucleotide variations between these related viruses are likely attributable to covariant substitutions throughout the entire IRES element of each respective virus, with maintenance of the overall tertiary structure as the critical factor. Nonetheless, the GGG trinucleotide sequences were maintained in each of the IRESs examined, with conservation of these sequences being critical for IRES activity in all the viral sequences tested except the unrelated HIV-1 Tar element (Fig. 8).

The HIV-1 Tar loop is an important recognition site for viral and cellular proteins which are required to facilitate transcriptional elongation of the HIV-1 genome (41). Recently, it has been shown that the Tar loop, including the apical GGG triplet, is an important element for the recognition of eukaryotic initiation factor 2 (3). The complete loss of function in an HCV/Tar-HIV-1 chimera would suggest that the HCV IIId loop does not perform a similar function in HCV translation. This is supported by earlier studies, which did not show interactions of IIId sequences with the 48S complex (23).

Previously it has been shown that cap-independent translation of the HCV IRES involves the direct recruitment of the 40S ribosomal subunit and eukaryotic initiation factor 3 (6, 23, 32). In an earlier study, we showed that single G-to-C mutations of the IIId apical loop can affect RNA folding in distinct patterns, yet all of these mutations result in complete loss of IRES function (18). This is due in part to an equal loss of affinity of each G-to-C point mutant for the 40S-ribosomal subunit (J. S. Kieft, K. Zhou, R. Jubin, and J. A. Doudna, submitted for publication). In addition, the correct secondary structure of IIId has also been suggested to be important for the binding of ribosomal protein S9 (22). IIId sequences and secondary structures are emerging as important factors for proper HCV IRES translation.

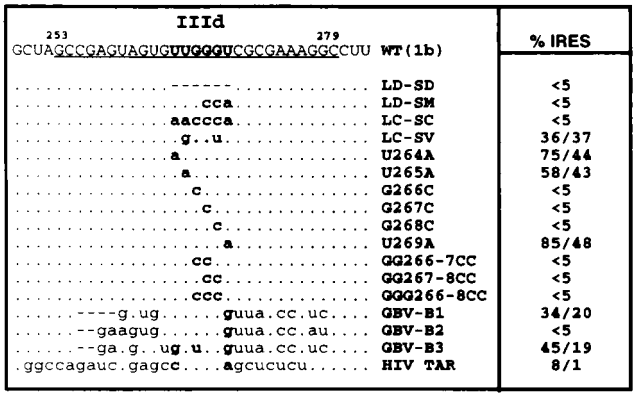

FIG. 8. Summary figure compiling IIId apical mutations and chimeras with their relative IRES translational efficiencies compared to wild-type HCV IRES. Annotations are the same as those listed in the legend to Fig. 5, except that apical loop sequences are listed in bold type. Percent IRES activity is shown on the right with results listed as in vitro- and cell-based results. Single values denote the same result in both in vitro- and cell-based assays.

RNase T_1 probing of various IRES constructs was used to detect changes in the secondary structure and possibly the tertiary structure that are induced by the introduction of mutations or chimeric sequences. The tendency for GBV-B2 to form alternate secondary structures is likely due to the presence of the internal asymmetric loop in the helical stem which could disrupt proper base pairing within the stem loop. The addition of magnesium changes the pattern of RNase T_1 cleavage of GBV-B2, but it does not restore wild-type folding (Fig. 7). Interestingly, the RNase T_1 cleavage pattern in the presence of magnesium indicates that the apical loop of IIId is forming, because the G nucleotides in the loop have become sensitive to cleavage. However, nucleotides upstream of IIId continue to be cleaved. It is possible that formation of this fold induces specific local tertiary structures that in turn lead to rearrangement of the secondary structure into a "more wild-type" structure. The rearrangement of secondary structures by tertiary-structure formation has been previously observed in other RNAs (42).

This study identified the IIId apical loop of the HCV IRES as an important region for IRES translation. Mutagenesis specifically identified the GGG (nucleotides 266 through 268) triplet of IIId as the region most critical for IRES function. The strong sequence conservation of this GGG triplet and chimeric HCV/IIId-GBV-B IRES activity suggests that a likely scenario exists among related flaviviruses and pestiviruses too. RNase T_1-probing results showed that the stem-loop IIId nucleotide sequence and local secondary structure can play a larger role in the correct folding of other regions of domain III that also contribute to proper IRES translation. In conclusion, the essentiality of IIId for translational activity and IRES folding strongly supports its validity as a specific target for the development of antiviral therapy.

ACKNOWLEDGMENTS

We are grateful to S. M. Lemon for the generous gift of the BT7-H cell line and helpful suggestions during our studies. We also thank M. Endres for critical reading of the manuscript.

REFERENCES

1. **Alt, M., R. Renz, P. H. Hofschneider, G. Paumgartner, and W. H. Caselmann.** 1995. Specific inhibition of hepatitis C viral gene expression by antisense phosphorothioate oligodeoxynucleotides. Hepatology **22:**707–717.
2. **Antivirals, Inc.** 1997. Technical bulletin no. 2. Antivirals, Inc., Corvallis, Oreg.
3. **Ben-Asouli, Y., Y. Banai, H. Hauser, and R. Kaempfer.** 2000. Recognition of 5′-terminal TAR structure in human immunodeficiency virus-1 mRNA by eukaryotic translation initiation factor 2. Nucleic Acids Res. **28:**1011–1018.
4. **Brown, E. A., H. Zhang, L. H. Ping, and S. M. Lemon.** 1992. Secondary structure of the 5′ nontranslated regions of hepatitis C virus and pestivirus genomic RNAs. Nucleic Acids Res. **20:**5041–5045.
5. **Bukh, J., R. H. Purcell, and R. H. Miller.** 1992. Sequence analysis of the 5′ noncoding region of hepatitis C virus. Proc. Natl. Acad. Sci. USA **89:**4942–4946.
6. **Buratti, E., S. Tisminetzky, M. Zotti, and F. E. Baralle.** 1998. Functional analysis of the interaction between HCV 5′UTR and putative subunits of eukaryotic translation initiation factor eIF3. Nucleic Acids Res. **26:**3179–3187.
7. **Caselmann, W. H., S. Eisenhardt, and M. Alt.** 1997. Synthetic antisense oligodeoxynucleotides as potential drugs against hepatitis C. Intervirology **40:**394–399.
8. **Choo, Q. L., G. Kuo, A. J. Weiner, L. R. Overby, D. W. Bradley, and M. Houghton.** 1989. Isolation of a cDNA clone derived from a blood-borne non-A, non-B viral hepatitis genome. Science **244:**359–362.
9. **Davidson, F., P. Simmonds, J. C. Ferguson, L. M. Jarvis, B. C. Dow, E. A. Follett, C. R. Seed, T. Krusius, C. Lin, G. A. Medgyesi, et al.** 1995. Survey of major genotypes and subtypes of hepatitis C virus using RFLP of sequences amplified from the 5′ non-coding region. J. Gen. Virol. **76:**1197–1204.
10. **Frolov, I., M. S. McBride, and C. M. Rice.** 1998. *cis*-acting RNA elements required for replication of bovine viral diarrhea virus-hepatitis C virus 5′ nontranslated region chimeras. RNA **11:**1418–1435.
11. **Hanecak, R., V. Brown-Driver, M. C. Fox, R. F. Azad, S. Furusako, C. Nozaki, C. Ford, H. Sasmor, and K. P. Anderson.** 1996. Antisense oligonucleotide inhibition of hepatitis C virus gene expression in transformed hepatocytes. J. Virol. **70:**5203–5212.
12. **Honda, M., L. H. Ping, R. C. Rijnbrand, E. Amphlett, B. Clarke, D. Rowlands, and S. M. Lemon.** 1996. Structural requirements for initiation of translation by internal ribosome entry within genome-length hepatitis C virus RNA. Virology **222:**31–42.
13. **Honda, M., E. A. Brown, and S. M. Lemon.** 1996. Stability of a stem-loop involving the initiator AUG controls the efficiency of internal initiation of translation on hepatitis C virus RNA. RNA **2:**955–968.
14. **Honda, M., M. R. Beard, L. H. Ping, and S. M. Lemon.** 1999. A phylogenetically conserved stem-loop structure at the 5′ border of the internal ribosome entry site of hepatitis C virus is required for cap-independent viral translation. J. Virol. **73:**1165–1174.
15. **Jaeger, J. A., and I. Tinoco, Jr.** 1993. An NMR study of the HIV-1 TAR element hairpin. Biochemistry **32:**12522–12530.
16. **Jubin, R., and M. G. Murray.** 1998. Activity screening of bacteria containing *Renilla* luciferase plasmids. BioTechniques **24:**185–188.
17. **Kamoshita, N., K. Tsukiyama-Kohara, M. Kohara, and A. Nomoto.** 1997. Genetic analysis of internal ribosomal entry site on hepatitis C virus RNA: implication for involvement of the highly ordered structure and cell type-specific transacting factors. Virology **233:**9–18.
18. **Kieft, J. S., K. Zhou, R. Jubin, M. G. Murray, J. Y. Lau, and J. A. Doudna.** 1999. The hepatitis C virus internal ribosome entry site adopts an ion-dependent tertiary fold. J. Mol. Biol. **292:**513–529.
19. **Kiyosawa, K., T. Sodeyama, E. Tanaka, Y. Gibo, K. Yoshizawa, Y. Nakano, S. Furuta, Y. Akahane, K. Nishioka, R. H. Purcell, et al.** 1990. Interrelationship of blood transfusion, non-A, non-B hepatitis and hepatocellular carcinoma: analysis by detection of antibody to hepatitis virus. Hepatology **4:**671–675.
20. **Lemon, S. M., and M. Honda.** 1997. Internal ribosomal entry sites within the RNA genomes of hepatitis C virus and other flaviviruses. Semin. Virol. **8:**274–288.
21. **Mizutani, T., N. Kato, M. Hirota, K. Sugiyama, A. Murakami, and K. Shimotohno.** 1995. Inhibition of hepatitis C virus replication by antisense oligonucleotide in culture cells. Biochem. Biophys. Res. Commun. **212:**906–911.
22. **Odreman-Macchioli, F. E., S. G. Tisminetzky, M. Zotti, F. E. Baralle, and E. Buratti.** 2000. Influence of correct secondary and tertiary RNA folding on the binding of cellular factors to the HCV IRES. Nucleic Acids Res. **28:**875–885.
23. **Pestova, T. V., I. N. Shatsky, S. P. Fletcher, R. J. Jackson, and C. U. Hellen.** 1998. A prokaryotic-like mode of cytoplasmic eukaryotic ribosome binding to the initiation codon during internal translation initiation of hepatitis C and classical swine fever virus RNAs. Genes Dev. **12:**67–83.
24. **Pestova, T. V., and C. U. Hellen.** 1999. Internal initiation of bovine diarrhea virus RNA. Virology **258:**249–256.
25. **Psaridi, L., U. Georgopoulou, A. Varaklioti, and P. Mavromara.** 1999. Mutational analysis of a conserved tetraloop in the 5′ untranslated region of hepatitis C virus identifies a novel RNA element essential for the internal ribosome entry site function. FEBS Lett. **453:**49–53.
26. **Reynolds, J. E., A. Kaminski, H. J. Kettinen, K. Grace, B. E. Clarke, A. R. Carroll, D. J. Rowlands, and R. J. Jackson.** 1995. Unique features of internal initiation of hepatitis C virus RNA translation. EMBO J. **14:**6010–6020.
27. **Reynolds, J. E., A. Kaminski, A. R. Carroll, B. E. Clarke, D. J. Rowlands, and R. J. Jackson.** 1996. Internal initiation of translation of hepatitis C virus RNA: the ribosome entry site is at the authentic initiation codon. RNA **2:**867–878.
28. **Rijnbrand, R., P. Bredenbeek, T. van der Straaten, L. Whetter, G. Inchauspe, S. Lemon, and W. Spaan.** 1995. Almost the entire 5′ non-translated region of hepatitis C virus is required for cap-independent translation. FEBS Lett. **365:**115–119.
29. **Rijnbrand, R. C., T. E. Abbink, P. C. Haasnoot, W. J. Spaan, and P. J. Bredenbeek.** 1996. The influence of AUG codons in the hepatitis C virus 5′ nontranslated region on translation and mapping of the translation initiation window. Virology **226:**47–56.
30. **Simmonds, P., E. C. Holmes, T. A. Cha, S. W. Chan, F. McOmish, B. Irvine, E. Beall, P. L. Yap, J. Kolberg, and M. S. Urdea.** 1993. Classification of hepatitis C virus into six major genotypes and a series of subtypes by phylogenetic analysis of the NS5 region. J. Gen. Virol. **74:**2391–2399.
31. **Simmonds, P., A. Alberti, H. J. Alter, F. Bonino, D. W. Bradley, C. Brechot, J. T. Brouwer, S. W. Chan, K. Chayama, D. S. Chen, et al.** 1994. A proposed system for the nomenclature of hepatitis C viral genotypes. Hepatology **19:**1321–1324.
32. **Sizova, D. V., V. G. Kolupaeva, T. V. Pestova, I. N. Shatsky, and C. U. Hellen.** 1998. Specific interaction of eukaryotic translation initiation factor 3 with the 5′ nontranslated regions of hepatitis C virus and classical swine fever virus RNAs. J. Virol. **72:**4775–4782.
33. **Summerton, J., D. Stein, S. B. Huang, P. Matthews, D. Weller, and M. Partridge.** 1997. Morpholino and phosphorothioate antisense oligomers compared in cell-free and in-cell systems. Antisense Nucleic Acid Drug Dev. **7:**63–70.
34. **Summerton, J., and D. Weller.** 1997. Morpholino antisense oligomers: design, preparation, and properties. Antisense Nucleic Acid Drug Dev. **7:**187–195.
35. **Tang, S., A. J. Collier, and R. M. Elliott.** 1999. Alterations to both the primary and predicted secondary structure of stem-loop IIIc of the hepatitis C virus 1b 5′ untranslated region (5′UTR) lead to mutants severely defective in translation which cannot be complemented in *trans* by the wild-type 5′UTR sequence. J. Virol. **73:**2359–2364.
36. **Tsukiyama-Kohara, K., N. Iizuka, M. Kohara, and A. Nomoto.** 1992. Internal ribosome entry site within hepatitis C virus RNA. J. Virol. **66:**1476–1483.
37. **Wakita, T., and J. R. Wands.** 1994. Specific inhibition of hepatitis C virus expression by antisense oligodeoxynucleotides: in vitro model for selection of target sequence. J. Biol. Chem. **269:**14205–14210.
38. **Wang, C., P. Sarnow, and A. Siddiqui.** 1993. Translation of human hepatitis C virus RNA in cultured cells is mediated by an internal ribosome-binding mechanism. J. Virol. **67:**3338–3344.
39. **Wang, C., P. Sarnow, and A. Siddiqui.** 1994. A conserved helical element is essential for internal initiation of translation of hepatitis C virus RNA. J. Virol. **68:**7301–7307.
40. **Wang, C., S. Y. Le, N. Ali, and A. Siddiqui.** 1995. An RNA pseudoknot is an essential structural element of the internal ribosome entry site located within the hepatitis C virus 5′ noncoding region. RNA **1:**526–537.
41. **Wei, P., M. E. Garber, S.-M. Fang, W. H. Fischer, and K. A. Jones.** 1998. A novel CDK9-associated c-type cyclin interacts directly with HIV-1 tat and mediates its high-affinity, loop-specific binding to tar RNA. Cell **92:**451–462.
42. **Wu, M., and I. Tinico, Jr.** 1998. RNA folding causes secondary structure rearrangement. Proc. Natl. Acad. Sci. USA **95:**11555–11560.